

**SHORT COMMUNICATION**

## **Open-Loop Fiber-Optic Gyroscope: A Technical Note**

M.H. Khan

*Hindustan Aeronautics Limited, Korwa*

and

C. Ramakrishna\*

*Institute of Armament Technology, Pune-411 025*

### **ABSTRACT**

This technical note describes the design and fabrication of a prototype open-loop interferometric fiber-optic gyroscope (IFOG). The gyro transfer function is transposed from that of a raised-cosine to a sine function using AC modulation, giving maximum sensitivity at rest. Among various signal processing methods, lock-in principle is used to detect the Sagnac phase shift due to rotation. Initial work is done with bulk-optic components. Finally, all-fiber gyroscope is built using laser diode (1300 nm), PINFET detector, fiber couplers and PZT phase modulator. An effort is made to develop compact IFOG with sensing coil diameter of 10 cm and signal processing card of size 10 x 6.5 sq cm. The present set-up is able to detect the direction of rotation at a rotation rate of  $5 \times 10^{-4}$  rad/s. Presently, the performance of the set-up is limited by the difficulty in achieving complete reciprocity.

### **1. INTRODUCTION**

All the optical gyroscopes are based on Sagnac effect<sup>1</sup>. They can be classified as active and passive (Fig. 1). Ring laser gyro is an active gyro whereas resonator and interferometric fiber-optic gyroscopes are passive in nature. Since the first report of fiber-optic rotation sensor by Vali and Shorthill<sup>2</sup>, many researchers followed the exciting subject which involves various domains of physics, electronics and technology to converge on a final design of relative simplicity.

To accurately measure the Sagnac phase shift, it is necessary to reduce other phase differences which can vary under the influence of environment; and the degree to which this is possible determines the quality of gyroscope. This is achieved by using the principle of reciprocity<sup>3</sup> to identically cancel the large unwanted drifts and to detect and measure reliably the small rotation-induced phase change. Once the reciprocal

configuration is adapted, the main subject of technological concern has been the 'heart' of the interferometer, composed of two beamsplitters, a polariser, a spatial single mode filter, and a modulator. It should allow maximum useful optical signal to ultimately reach the detector and lend itself to non labour intensive mass production.

### **2. SYSTEMS**

The fiber-optic gyroscope can be built using three technologies:

- (a) Bulk-optic hybrid gyroscope,
- (b) All-fiber gyroscope, and
- (c) Integrated-optic hybrid gyroscope.

To achieve a wide dynamic range with good linearity, many demodulation systems have been proposed. These systems can be classified into two

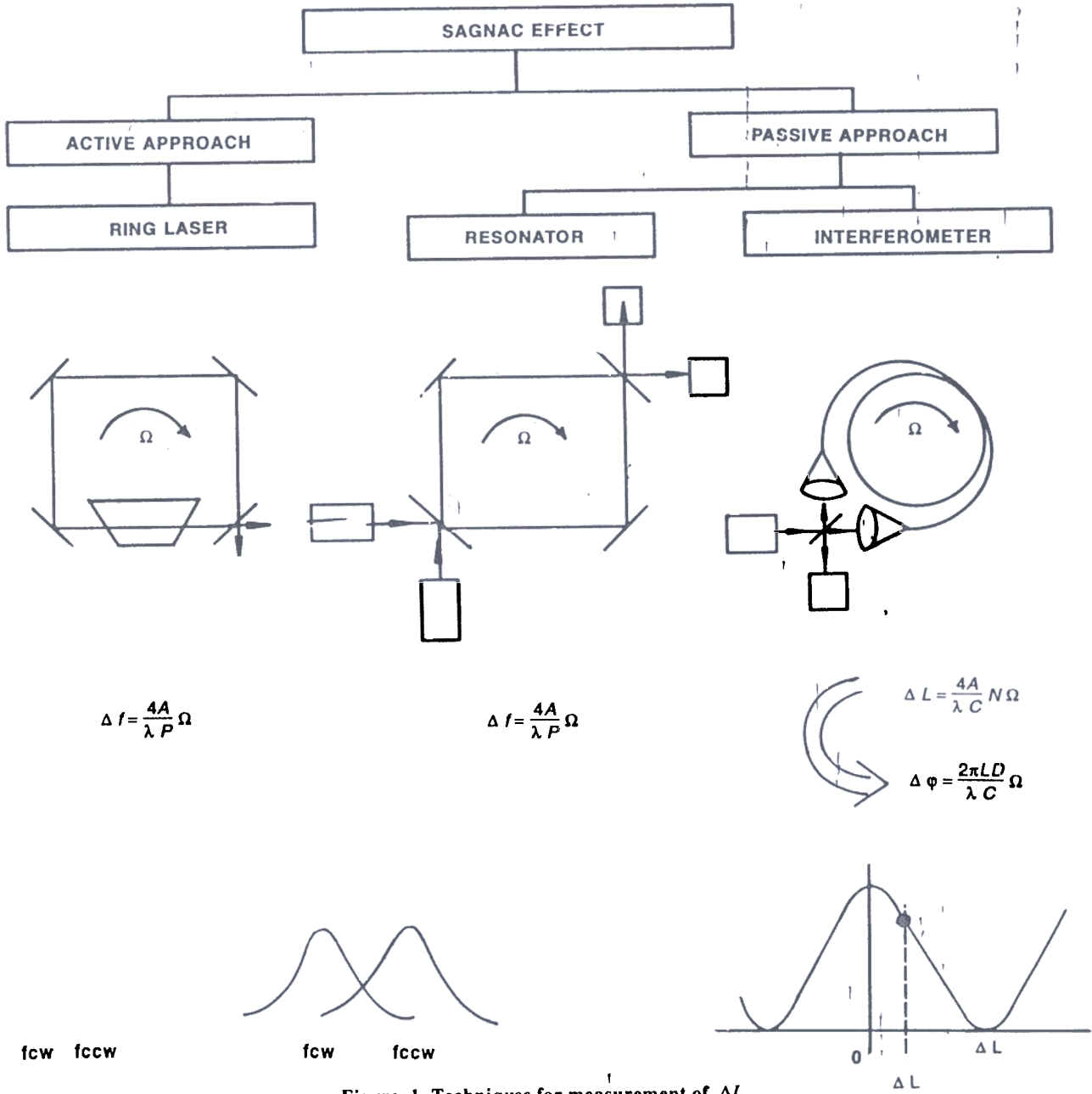


Figure 1. Techniques for measurement of  $\Delta L$ .

categories: open loop and closed loop systems. The open loop<sup>4</sup> system approach is used here. In open loop systems, the demulated output is a sinusoidal function of  $\delta \phi_s$ , the Sagnac phase shift. The disadvantages of the open loop system are:

- (a) The output signal is nonlinear function of the rotation rate with dynamic range limited by the sinusoidal waveform.
- (b) The output is in the form of an analog electrical current.

- (c) The stability of the optical power,  $P_o$  of the light sources and the scale factor are questionable. The scale factor linearity becomes worse as the rotation rate increase.
- (d) This approach is limited by the stability of the analog circuits.

Though various approaches are reported to increase the dynamic range and the scale factor linearity of the gyroscope, this study is limited to the present work due to the limitations in the availability of

components. In a paper presented at the 20th OSI Symposium conducted at SAMEER, Bombay, the authors had reported the bulk-optic hybrid gyroscope which could demonstrate the principle, and after gaining confidence, the authors attempted the development of all fiber gyroscope<sup>5</sup>, which is described here.

### 3. ALL-FIBER OPEN LOOP GYROSCOPE

In this set-up, the following components are used:

- (a) Sensing coil having average diameter 79 mm
- (b) Ordinary communication grade SMF (OPTEL make) having cut-off wavelength = 1.2  $\mu$ m.
- (c) Length of fiber used,  $L = 571$  m
- (d) Phase modulator, PZT type 5A, having mechanical radial resonance frequency of 30 kHz.
- (e) Optical source: Lasertron make laser diode QLM 1300 SM 565,  $\lambda = 1300$  nm, output power 300  $\mu$ W.
- (f) Detector: Lasertron make QDFT PINFET, with  $R > 0.8$  A/W at 1300 nm.
- (g) 3dB couplers: DC1 with TR ratio 47.4/52.6 and DC2 with TR ratio 50.6/49.4.
- (h) FET input operational amplifier LF356 used for amplification and filters
- (i) Analog multiplier AD534 used for demodulation. The block diagram and the layout of this set-up are shown in Figs 2 and 3.

The Sagnac scale factor for this set-up is

$$K_s = 2 LD/C$$

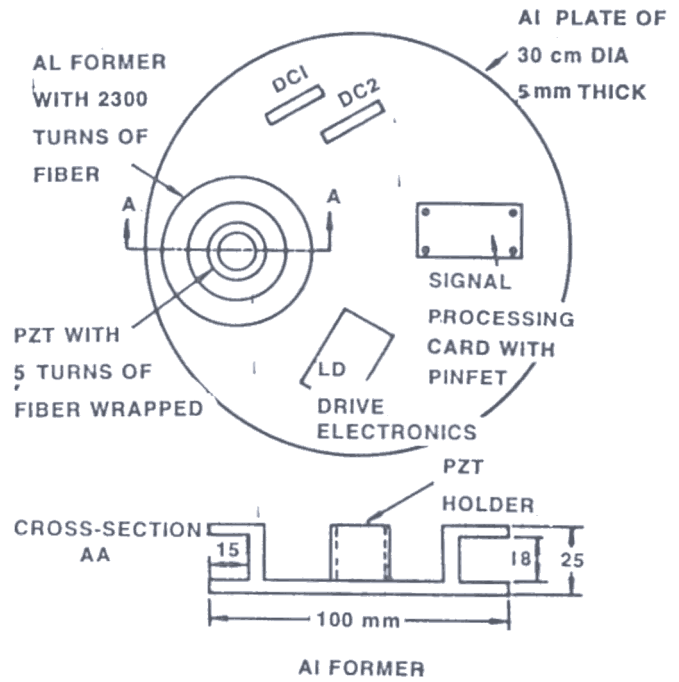


Figure 3. Layout of all-fiber gyro.

$$K_s = 3.54 \mu\text{rad/deg/h}$$

$$= 0.73 \text{ arc-s/(deg/h)}$$

Hence for rotation rate of 10 deg/h, the Sagnac phase shift  $\delta \phi_s$  will be 35.4  $\mu$ rad.

Uncertainty in the measurement of  $\Omega$  under photon shot noise limit conditions with  $n_{ph} = 3 \times 10^{19}$  photon/s (corresponding to 10  $\mu$ W),  $n_D = 0.7$ ,  $\tau = 1$  s, will be

$$\delta(\Omega) = 0.94 \mu\text{rad/s or } 0.2 \text{ deg/h}$$

Hence, under photon shot noise limited conditions, we can sense the rotation rate of 0.2 deg/h with this set-up.

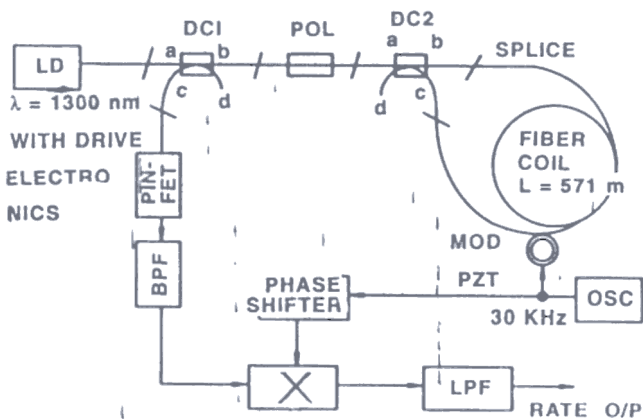


Figure 2. Block diagram of experimental set-up using all-fiber configuration.

phase shift in sinusoidal wave form which is filtered out by a low pass filter (LPF).

The output from directional coupler, DC1 (Fig. 2), is coupled to PINFET detector which has responsivity greater than 0.8 A/W at 1300 nm and built-in pre-amplifier. PINFET is connected to a load resistance  $R_1 = 1.5 \text{ K}$ . The output of the PINFET pre-amplifier is fed to a infinite-gain multiple feedback band pass filter (BPF). This circuit is useful for  $Q \leq 10$ . The component values have been selected for  $Q = 10$ , gain = 5 and center frequency 30 kHz. The values of resistors and capacitors are  $R_2 = 10 \text{ K ohm}$ ,  $R_3 = 273 \text{ ohm}$ ,  $R_4 = R_5 = 106 \text{ K ohm}$ , and  $C_1 = C_2 = 0.001 \text{ F}$ . Actual practical values of components used are indicated in Fig. 4. This BPF was built by using LF356.

The reference signal for demodulation is derived from signal generator which is fed to a buffer amplifier with variable gain (IC used LF356). Resistor values for this amplifier are  $R_9 = 4.7 \text{ K ohm}$ ,  $R_{10} = 10 \text{ K ohm}$  and  $R_{11} = 100 \text{ K ohm}$  variable. The output of this stage is then fed to a phase shifter. The phase can be continuously varied from 0 to  $180^\circ$  by variable resistor  $R_{14}$ . Actual component values of this phase shifter are  $R_{12} = R_{13} = 10 \text{ K ohm}$ ,  $C_4 = 0.01 \mu\text{F}$  and  $R_{14} = 1 \text{ K ohm}$  variable. The output of this phase shifter is fed to  $Y_1$  input of multiplier through a coupling capacitor  $C_5$ .

The analog multiplier AD534 has been used which is a four quadrant multiplier/divider. The output is given by  $V_z = V_{x1} * V_{y1} / 10$ . The output will contain *dc* term corresponding to Sagnac phase shift and harmonics of

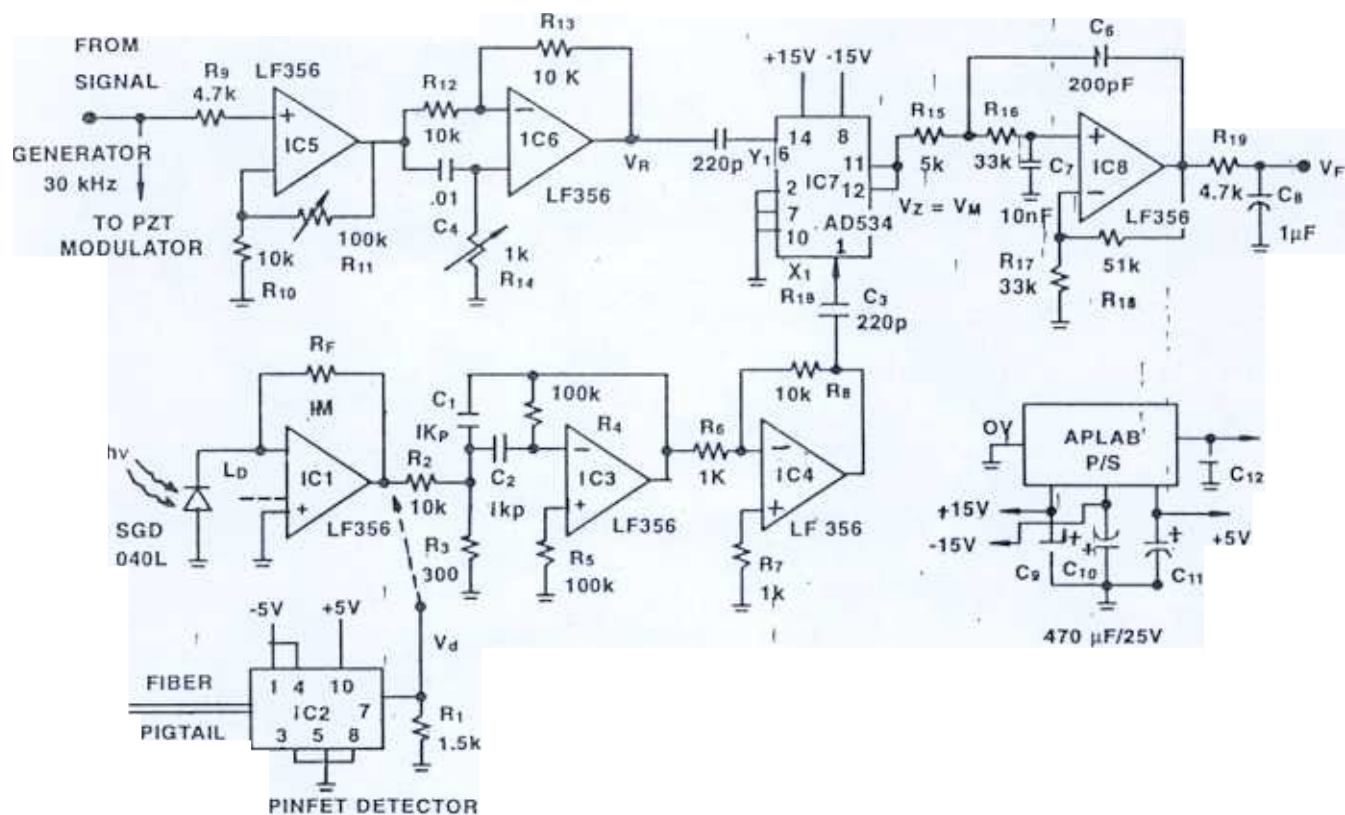


Figure 4. Signal processing scheme.

The output of this BPF is given to an amplifier in inverting configuration (IC used LF 356) with gain of 10. The resistor values are  $R_6 = R_7 = 1 \text{ K ohm}$  and  $R_8 = 10 \text{ K ohm}$ . The output is fed to X input of multiplier through a coupling capacitor  $C_3$ .

modulating frequency. These harmonics are filtered out by an LPF with cut-off frequency much below the modulating frequency. The output of LPF will correspond to Sagnac phase shift due to a given rotation rate. The LPF is (IC used LF 356) a second order low

pass Butterworth VCVS filter<sup>6</sup>. The practical values of components are  $R_{15} = 5 \text{ K ohm}$ ,  $R_{16} = R_{17} = 33 \text{ K ohm}$ ,  $R_{18} = 51 \text{ ohm}$ ,  $C_6 = 200 \text{ PF}$  and  $C_7 = 10 \text{ nF}$ . This circuit has a gain of 2.5 and cut-off frequency 100 Hz. A passive LPF also has been used to further attenuate harmonic components.

All these components have been mounted on a PCB of  $10 \times 6.5 \text{ sq cm}$  to have a compact gyro.

## 5. OPTICAL CIRCUIT & PHASE MODULATOR

Input and output (port 'a' and 'c' of DC1) are connected through connectors to LD and PINFET, respectively (Fig. 2). Both ends of fiber coil are spliced to ports 'b' and 'c' of DC2. Port 'b' of DC1 and port 'a' of DC2 are spliced together. Port 'd' of both are radiating ports and are left free. Due to its non-availability, the fiber polariser was not used although it is shown in the diagram. The LD is used with built-in drive circuit which needs P/S of +5 V and -12 V. The excess loss of DC1 and DC2 is around 0.5 dB.

Phase modulator is made by wrapping five turns of fiber around a cylindrical PZT with dimensions O.D = 33 mm and height = 20mm. It is driven at modulating frequency of 30 kHz from a signal generator. This modulator is mounted with the help of specially fabricated holder. No significant loss was noticed due to this modulator.

The 571 m long fiber with  $N = 2300$  turns is tightly wound on an aluminium former with coil winding machine. Simple winding (not quadrupolar) was done. The loss due to fiber coil was measured was around -0.21 dB.

The total loss of circuit was measured to be around -11 dB. Hence, with LD output of  $300 \mu\text{W}$ , the expected power which reaches the detector will be around  $2 \mu\text{W}$ .

## 6. MECHANICAL DESIGN

In this set-up, the mechanical design was greatly simplified compared to bulk optic version where design and fabrication of micropositioner were complicated. The mechanical components of the present set-up are aluminium former, PZT holder and an aluminium disc for mounting the components. The diameter of former is reduced to 10 cm with 15 mm of groove cut for winding the fiber. The PZT holder is made of MS with diameter of 27 mm and height of 20 mm. The PZT is directly mounted in the holder at the center of the

former. The whole system is mounted on aluminium disc of 30 cm diameter. An effort has been made to bring the size closer to practical gyro.

## 7. RESULTS

The performance of all fiber gyroscopes was greatly improved in comparison to that in case of bulk optic approach. The output signal was fairly stable. Due to nonavailability of fiber polariser and other noise sources, e.g., backscattering from fiber, nonlinear Kerr effect, Faraday effect, earth rotation and parasitic transient effects, there was a small signal without giving any rotation. It will give a fixed bias error. It is very much dependent on the layout of extra fiber loops between the components. Slow variation in drift was noticed, which may be probably due to temperature change and coupling of orthogonal polarisation modes.

With all these error sources and drift, a slow rotation rate of the system either CW or CCW produced corresponding output signal in opposite polarity sensing the direction of rotation. Rough estimate gives the bias stability of around  $5 \times 10^{-4} \text{ rad/s}$  for this set-up. In our view, by using fiber polariser, an improvement of two orders can be easily achieved. To achieve high accuracy and sensitivity approaching photon noise limited conditions further work is required in minimising error sources as mentioned above. One of the error sources namely the effect due to back scatter can be minimised by replacing the laser diode with an SLD (super luminescent diode). Open-loop IFOG will be suitable for the applications that need limited dynamic range and scale factor accuracy. One of the applications is in the attitude and heading reference system (AHRS) in aircrafts. Dornier DL 328 will be the first airliner to use a fiber-optic gyro AHRS unit. Compact commercial systems are being produced by Andrew Corporation, USA.

## REFERENCES

- Post, E. J. Sagnac effect. *Rev. Mod. Phys.* 1967, 39, 475-94.
- Vali, V. & Shorthill, R.W. Fiber ring interferometer. *Applied Optics*, 1976, 15, 1099-1100.
- Bergh, R.A.; Lefevre, H.C. & Shaw, H.J. An overview of fiber-optic gyroscopes. *J. Lightwave Tech.*, 1984, 2(2), 91-107.
- Liu, R.Y. & Adams, G.W. Interferometric fiber-optic gyroscopes: A summary of progress, IEEE position location and navigation symposium, 1990. pp 31-35.

5. Lefevre, H.C. Fiber-optic gyroscope. *In* Fiber-optic sensor: Systems and applications edited by B. Culshaw and J. Dakin. Artech House Inc. Norwood, 1989. pp. 381-425.
6. Johnson, D.E. & Hilburn, J.L. *In* Rapid practical designs of active filters. John Wiley & Sons, Inc. 1975. p. 11.

## Contributors



**Shri MH Khan** completed his BE (Electronics & Communication) from University of Roorkee in 1983 and joined Hindustan Aeronautics Limited. He completed his MTech (Lasers & Electrooptics) from Institute of Armament Technology, Pune in 1993 and Diploma in Management from Indira Gandhi National Open University, New Delhi, in 1994. Presently, he is working in Design Department as Manager (Design). The areas of his interest are ring laser and fibre-optic gyros.

**Prof C Ramakrishna** received his MSc in Physics in 1962 from Sri Venkateswara University, Tirupati. Later, he received his MTech in Lasers & Electrooptics from the University of Poona, in 1990. Presently, he is Professor at the Faculty of Applied Physics, Institute of Armament Technology, Pune. His recent interests include : fiber-optics, carbondioxide lasers, semiconductor lasers, laser communication and semiconductor diode-pumped *ND:YAG* lasers.